JUSTC

Article

http://justc.ustc.edu.cn

Received: February 02, 2024; Accepted: March 22, 2024

An efficient strategy for the preparation of MIL-53(Al)-NH_2 membranes with high ion selectivity and desalination performance

Wenmin Li[1], Zheng Liu[1], Xingya Li[1], Rongqiang Fu[2], Zhaoming Liu[2], Tingting Xu[1] ✉, and Tongwen Xu[1] ✉

[1]*Key Laboratory of Precision and Intelligent Chemistry, Department of Applied Chemistry, School of Chemistry and Materials Science, University of Science and Technology of China, Hefei 230026, China;*
[2]*Shandong Tianwei Membrane Co., Ltd., Weifang 261061, China*

✉Correspondence: Tingting Xu, E-mail: xutt49@ustc.edu.cn; Tongwen Xu, E-mail: twxu@ustc.edu.cn

Graphical abstract

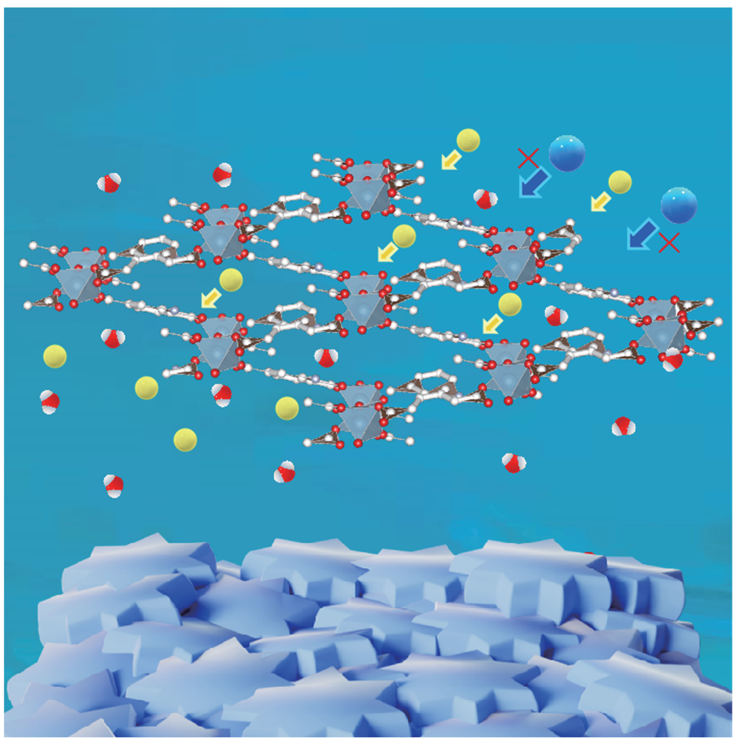

MIL-53(Al)-NH_2 membranes fabricated via a secondary growth strategy exhibit high ion selectivity and desalination performance.

Public summary

■ The MIL-53(Al)-NH_2 membranes were successfully prepared within a short time by a secondary growth strategy.

■ The fabricated membranes containing angstrom-scale (~7 Å) channels provide transport pathways for small monovalent ions and water molecules but hinder divalent cations.

■ The MIL-53(Al)-NH_2 membranes exhibit excellent ion separation performance (a selectivity of 121.42 for Na^+/Ca^{2+} and 93.81 for Li^+/Mg^{2+}) and desalination performance (a water/salt selectivity of up to 5196).

Citation: Li W M, Liu Z, Li X Y, et al. An efficient strategy for the preparation of MIL-53(Al)-NH_2 membranes with high ion selectivity and desalination performance. *JUSTC*, **2024**, 54(6): 0606. DOI: 10.52396/JUSTC-2024-0016 http://justc.ustc.edu.cn

Article

Received: February 02, 2024; Accepted: March 22, 2024

An efficient strategy for the preparation of MIL-53(Al)-NH_2 membranes with high ion selectivity and desalination performance

Wenmin Li[1], Zheng Liu[1], Xingya Li[1], Rongqiang Fu[2], Zhaoming Liu[2], Tingting Xu[1] ✉, and Tongwen Xu[1] ✉

[1]*Key Laboratory of Precision and Intelligent Chemistry, Department of Applied Chemistry, School of Chemistry and Materials Science, University of Science and Technology of China, Hefei 230026, China;*
[2]*Shandong Tianwei Membrane Co., Ltd., Weifang 261061, China*

✉Correspondence: Tingting Xu, E-mail: xutt49@ustc.edu.cn; Tongwen Xu, E-mail: twxu@ustc.edu.cn

Cite This: *JUSTC*, **2024**, 54(6): 0606 (7pp)   Read Online   Supporting Information

Abstract: The efficient extraction of sodium (Na^+) and lithium (Li^+) from seawater and salt lakes is increasingly demanding due to their great application value in chemical industries. However, coexisting cations such as divalent calcium (Ca^{2+}) and magnesium (Mg^{2+}) ions are at the subnanometer scale in diameter, similar to target monovalent ions, making ion separation a great challenge. Here, we propose a simple and fast secondary growth method for the preparation of MIL-53(Al)-NH_2 membranes on the surface of anodic aluminum oxide. Such membranes contain angstrom-scale (~7 Å) channels for the entrance of small monovalent ions and water molecules, endowing the selectivities for monovalent cations over divalent cations and water over salt molecules. The resulting high-connectivity MIL-53(Al)-NH_2 membranes exhibit excellent ion separation performance (a selectivity of 121.42 for Na^+/Ca^{2+} and 93.81 for Li^+/Mg^{2+}) and desalination performance (a water/salt selectivity of up to 5196). This work highlights metal-organic framework membranes as potential candidates for realizing ion separation and desalination in liquid treatment.

Keywords: metal-organic framework; MIL-53(Al)-NH_2; membrane; ion selectivity; desalination

CLC number: TQ051.8   **Document code:** A

1 Introduction

The extraction and separation of valuable metal ions in nature, for example, sodium/calcium (Na^+/Ca^{2+}) separation from seawater and lithium/magnesium (Li^+/Mg^{2+}) separation from salt lakes, is essential because of the increasing demand in daily production[1–4]. However, the similar physicochemical properties and diameters of coexisting cations make the separation process a great challenge[5–8]. In addition, the content of Li^+ in salt lakes is much lower than that of Mg^{2+}, which increases the difficulty of separation[9–11]. Thus, separation technologies require novel and effective designs to meet the growing demand for valuable metal ions.

For the past few years, membrane separation processes have been widely used for the extraction of Na^+ and Li^+ by size-sieving effect[12–14], electrostatic repulsion[15–17], and affinity difference[7, 18, 19]. The size-sieving effect is dominant among these separation mechanisms, which means that species smaller than the pores can permeate through the membrane, while larger species are screened out[12, 20–22]. However, the pores of traditional membranes fabricated via chemical crosslinking and acid–base reactions have a broad distribution, which is not conducive to separation and results in low selectivity[23–25]. For the precise construction of membrane pores, advanced polycrystalline microporous frameworks such as metal-organic frameworks (MOFs) are employed to fabricate separation membranes due to their regular pore structure and uniform pore size distribution[13, 26–28]. With their proper pores, MOFs have been employed in membrane fabrication and have shown decent potential for ion-selective transport, such as F^-/Cl^-, Br^-/NO_3^-, H^+/Cl^-, and Li^+/Mg^{2+}[7, 8, 29, 30]. Li et al.[31] successfully constructed PET-UiO-66-X (X = H, NH_2, and $N^+(CH_3)_3$) channels, which showed ultrahigh F^- conductivity and F^-/Cl^- selectivity. However, the PET substrate is complicated to handle and only has a single channel; thus, it is difficult to prepare continuous and dense membranes by this membrane fabrication strategy. Currently, several MOF membranes have been fabricated with excellent ion separation performance but still require a long growth time and the use of many organic solvents during the MOF layer growth process[21, 32, 33]. For instance, our group reported leaf-like UiO-66-NH_2 membranes[34] with excellent cation separation performance (Na^+/Mg^{2+} > 200 and Li^+/Mg^{2+} > 60), which required a long membrane formation time of 24 h/48 h, and *N*,*N*-dimethylformamide was used as the reaction solvent.

Herein, we report a high-connectivity MIL-53(Al)-NH_2 membrane without cracks fabricated by a simple and fast secondary growth method (Fig. 1). 2-Aminoterephthalic acid (2-NH_2-BDC) was used to pretreat the AAO substrate for the presynthesis of MIL-53(Al)-NH_2, followed by a secondary growth process with a short growth time. The crack-free

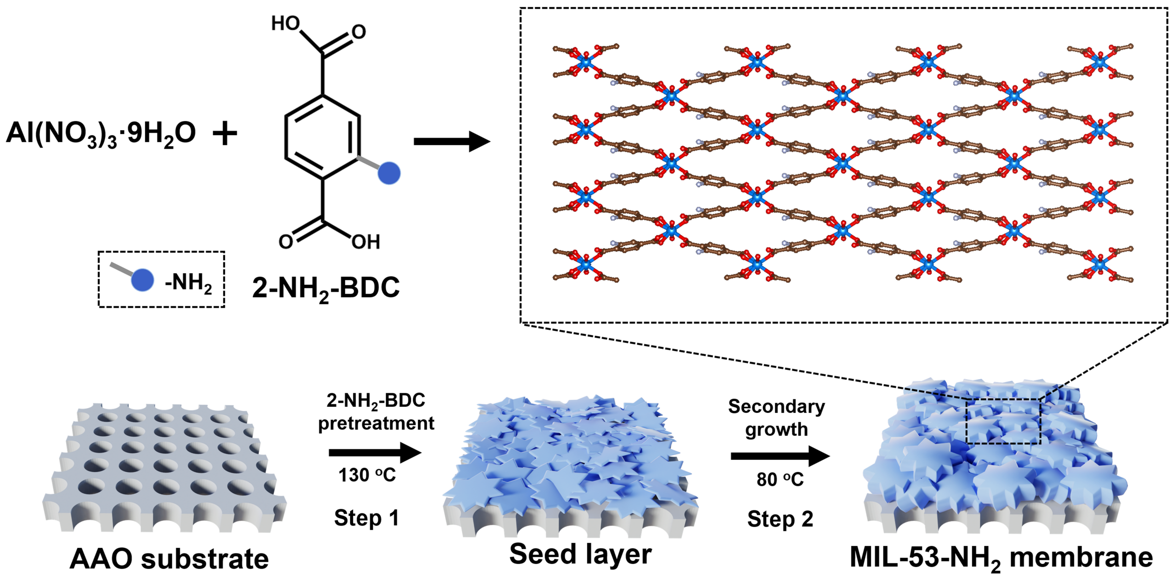

Fig. 1. Scheme of the fabrication of MIL-53(Al)-NH_2 membranes via the secondary growth method.

MOF layer grew firmly on the AAO substrate, which was confirmed by the SEM image. MIL-53(Al)-NH_2 with angstrom -scale (~7 Å)[30, 35, 36] apertures provides transport pathways for ions with small diameters and water molecules (~2.80 Å)[37] and hinders ions with large diameters. Therefore, the resultant MIL-53(Al)-NH_2 membranes show outstanding cation separation and desalination performance. For ion separation, the Na^+/Ca^{2+} and Li^+/Mg^{2+} selectivities are 121.42 and 93.81, respectively, which are much greater than the ion selectivity of the AAO substrate. In addition, the water/salt selectivity reached 5196, which is 230 times greater than that of the AAO substrate.

2 Results and discussion

2.1 Fabrication of the MIL-53(Al)-NH_2 membranes and powders

MIL-53(Al)-NH_2 membranes were fabricated on AAO substrates via a fast secondary growth method, which was carried out in a self-designed Teflon holder. The AAO disks with a pore size of 90 nm±10 nm and diameter of 25 mm were used as the substrate to support the MOF layer. In addition, the AAO substrate was also employed as the metal source for Al^{3+} to form the initial MIL-53(Al)-NH_2 seeding. Briefly, the AAO substrate was first preprocessed to presynthesize MIL-53(Al)-NH_2 seeds (MIL-53-NH_2-M-S). 2-Aminoterephthalic acid (2-NH_2-BDC) was used to pretreat the AAO substrate at 130 °C for 30 min (Fig. 1-step 1) to form MIL-53-NH_2-S. After the temperature cooled to room temperature, MIL-53-NH_2-M-S was reacted with $Al(NO_3)_3·9H_2O$ and 2-NH_2-BDC (Fig. 1-step 2) to prepare the MIL-53(Al)-NH_2 membrane. During the secondary growth process, crystallization occurred, and a continuous and defect-free membrane rapidly formed after 30 min and 60 min at 80 °C for MIL-53-NH_2-M-1 and MIL-53-NH_2-M-2, respectively. The synthesized MIL-53(Al)-NH_2 crystals had pore diameters of ~7 Å (Fig. 1). Scanning electron microscopy (SEM) images show that the MOF membrane morphology evolves with different growth times (Fig. 2). SEM images of the surface and cross-sections of MIL-53-NH_2-M-S, MIL-53-NH_2-M-1, and MIL-53-NH_2-M-2 confirmed that a continuous MOF layer was successfully formed on the surface of the AAO substrate even though the process experienced a short reaction time. The thickness of the MOF membranes increases with increasing growth time from 0.74 μm to 0.97 μm. From the Fourier transform infrared (FTIR) spectra (Fig. 3), the vibrational bands at 1654 cm^{-1} and 1579 cm^{-1} represent –C=O and –CO–NH, respectively, confirming that MIL-53(Al)-NH_2 was generated on the AAO substrate[38, 39]. X-ray diffraction (XRD) patterns of the MIL-53(Al)-NH_2 membranes and powders were measured to verify the crystallinity of the fabricated MOF materials. For MIL-53-NH_2-M-2, the X-ray diffraction (XRD) patterns (Fig. 3b) are basically consistent with the simulated pattern, demonstrating the high crystallinity of the fabricated MOF membranes[40]. However, the crystallinity of MIL-53-NH_2-M-S and MIL-53-NH_2-M-1 is not good, which may be caused by the short membrane growth time. Thus, the XRD patterns of the MIL-53(Al)-NH_2 powders were obtained to determine their crystallinity (Fig. 3c). Both of the XRD patterns for MIL-53-NH_2-P-1 and MIL-53-NH_2-P-2 are consistent with the simulated MIL-53(Al)-NH_2 pattern.

2.2 Ion transport properties of MIL-53(Al)-NH_2 membranes

The ion transport properties of the MIL-53(Al)-NH_2 membranes were measured under concentration-driven diffusion. The membranes were mounted on a homemade U-cell device, and the feed chamber and permeate chamber were separated (Fig. 4a). For the AAO substrate, the cation permeation rates of the single-ion system follow the order of K^+ (5.75 $mol·m^{-2}·h^{-1}$) > Na^+ (3.78 $mol·m^{-2}·h^{-1}$) > Li^+ (3.27 $mol·m^{-2}·h^{-1}$) > Mg^{2+} (2.97 $mol·m^{-2}·h^{-1}$), as shown in Fig. 4b, depending on the sequence of hydrated ion diameters[5]. The AAO substrates exhibit high permeation rates due to their much larger channel diameter (90 nm±10 nm) than the hydrated diameter

DOI: 10.52396/JUSTC-2024-0016
JUSTC, **2024**, 54(6): 0606

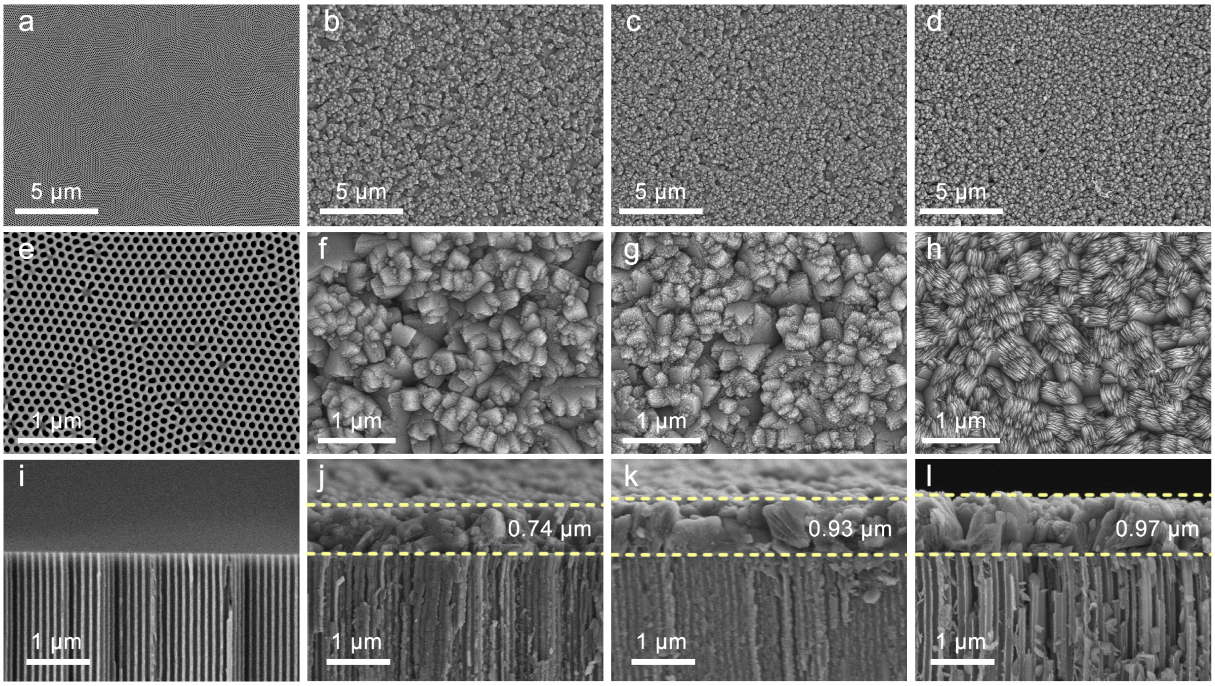

Fig. 2. SEM images of the AAO substrate and MIL-53(Al)-NH_2 membranes. SEM images of the surfaces of the AAO substrate (a), MIL-53-NH_2-M-S (b), MIL-53-NH_2-M-1 (c), and MIL-53-NH_2-M-2 (d) at low magnification. High-magnification SEM images of the surfaces of the AAO substrate (e), MIL-53-NH_2-M-S (f), MIL-53-NH_2-M-1 (g), and MIL-53-NH_2-M-2 (h). SEM cross-sectional images of the AAO substrate (i), MIL-53-NH_2-M-S (j), MIL-53-NH_2-M-1 (k), and MIL-53-NH_2-M-2 (l).

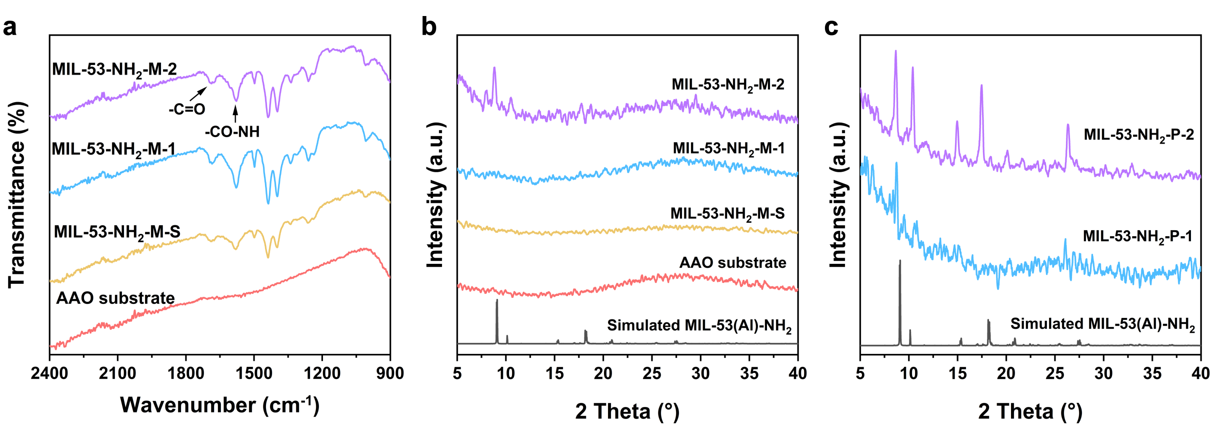

Fig. 3. FTIR spectra and XRD patterns of AAO and MIL-53(Al)-NH_2. (a) Fourier transform infrared (FTIR) spectra of the AAO and MIL-53(Al)-NH_2 membranes. (b) XRD patterns of the AAO substrate and MIL-53(Al)-NH_2 membranes. (c) XRD patterns of MIL-53(Al)-NH_2 powders.

of the cations. The calculated ideal Na^+/Ca^{2+} and Li^+/Mg^{2+} selectivities of the AAO substrate are 1.76 and 1.27, respectively (Fig. 4b). The limited ion selectivity of the AAO substrate indicates that the substrate has a negligible impact on the ion transport behavior.

After the growth of the MIL-53(Al)-NH_2 seedings on the AAO substrate, the permeation rates of cations in the MIL-53-NH_2-M-S membranes decreased substantially compared with those in the bare AAO substrate. For instance, the permeation rate of Na^+, which has the smallest hydrated diameter among the studied ions, decreased from 5.74 $mol·m^{-2}·h^{-1}$ for the bare AAO substrate to 0.22 $mol·m^{-2}·h^{-1}$ for the MIL-53-NH_2-M-S membrane. Other ion permeation rates are also reduced by orders of magnitude. The decreased cation permeation rates of the MIL-53(Al)-NH_2 membranes can be attributed to the decrease in the transport channel size from 90 nm±10 nm for the AAO substrate to 7 Å for the MIL-53(Al)-NH_2 membranes. Compared with those of the AAO substrate, the Na^+/Ca^{2+} and Li^+/Mg^{2+} selectivities of the MIL-53-NH_2-M-S membranes increased to 5.71 and 3.66, respectively. For the MIL-53-NH_2-M-1 and MIL-53-NH_2-M-2 membranes, as the growth time of the MOF layer increased, the ion flux continued to decrease. This is because the MOF layer becomes tighter. Specifically, the MIL-53-NH_2-M-2 membranes show low permeation rates of monovalent cations of 0.012 and 0.006 $mol·m^{-2}·h^{-1}$ for Na^+ and Li^+, respectively. The permeation rates of Ca^{2+} and Mg^{2+} for the MIL-53-NH_2-M-2 membranes decreased to 1.01×10^{-4} and 6.31×10^{-5} $mol·m^{-2}·h^{-1}$, respectively. The permeation rates of divalent cations decrease substantially compared to those of monovalent

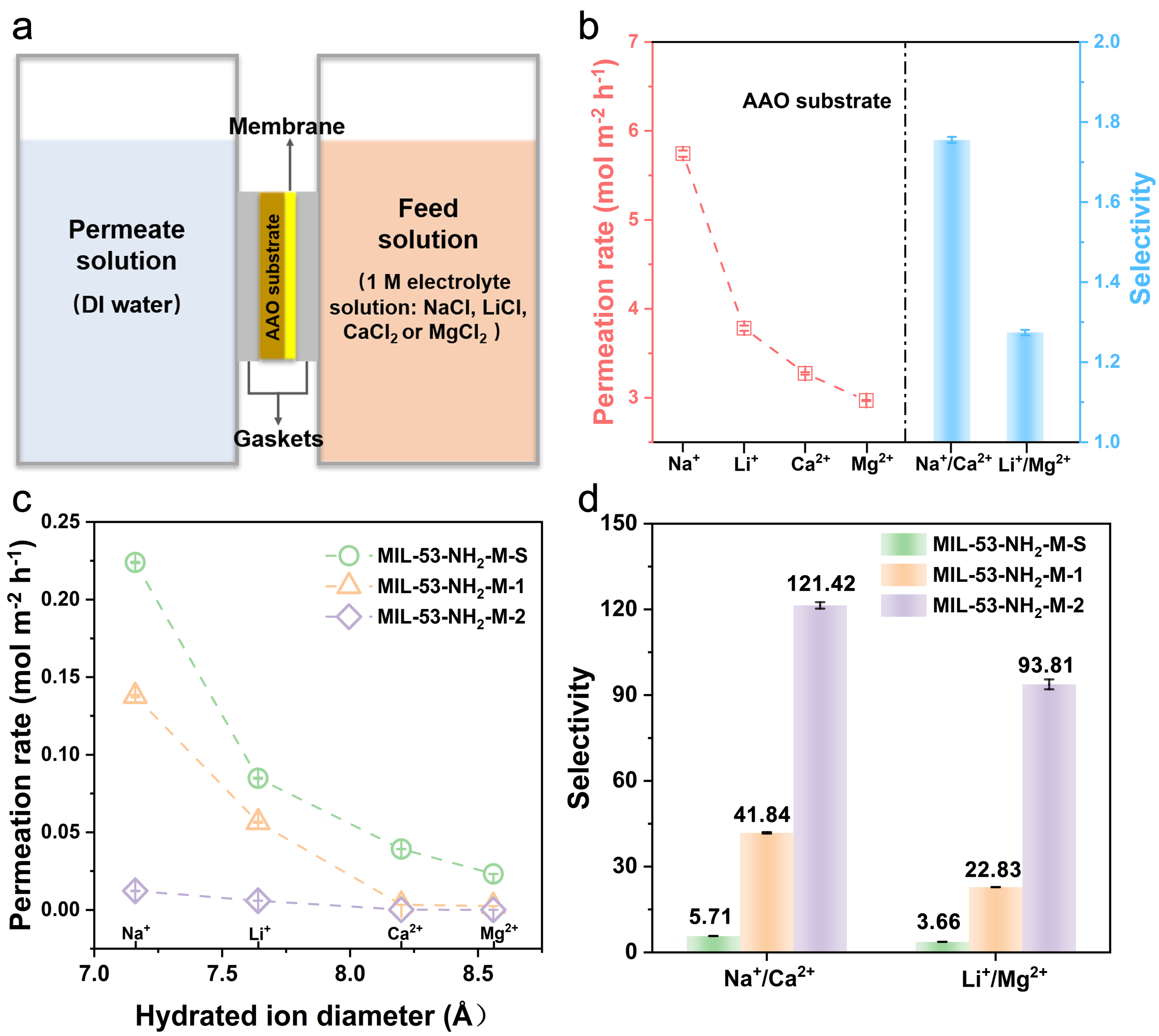

Fig. 4. Ion separation performance of MIL-53(Al)-NH_2 membranes. (a) The homemade U-cell device for the tests of ion separation performance. (b) The ion permeation rate and selectivity of the AAO substrate. (c) The ion permeation rates of MIL-53(Al)-NH_2 membranes. (d) The selectivities for Na^+/Ca^{2+} and Li^+/Mg^{2+} of MIL-53(Al)-NH_2 membranes.

cations, resulting in increased selectivity for monovalent cations over divalent cations (i.e., Na^+/Ca^{2+} selectivity and Li^+/Mg^{2+} selectivity). The Na^+/Ca^{2+} selectivity and Li^+/Mg^{2+} selectivity of MIL-53-NH_2-M-2 were 121.42 and 93.81, respectively. In particular, the selectivity of the MIL-53-NH_2-M-2 membrane is more than twenty times that of the MIL-53-NH_2-M-S membrane.

2.3 Water desalination performance

Considering the extremely low cation permeation rates of the fabricated MIL-53(Al)-NH_2 membranes, we further selected a simple water desalination experiment to investigate the permeation rates of salt (i.e., 1 mol·L^{-1} NaCl) and water for the membranes (Fig. 5a). For the AAO substrate, the pore size (90 nm±10 nm) is much larger than the size of the molecules, leading to the optional transport of water and salt molecules through the substrate. As a result, the concentration difference between the feed side and the draw side decreases, and the water migration slows, resulting in a low water/salt selectivity of 22.24. For MIL-53(Al)-NH_2 membranes, although the growth time of the MIL-53(Al)-NH_2 layer is quite short, the resulting MOF membranes composed of high-connectivity MOF crystals show excellent desalination performance. As the diameter of a water molecule (2.80 Å) is much smaller than that of a hydrated ion, water molecules can pass through breezily, whereas salt molecules are rejected by MOF channels with an aperture size of 7 Å[5, 30, 36]. The water and salt molecule fluxes for the studied membranes gradually increased with increasing growth time. Therefore, the MIL-53-NH_2-M-2 membrane exhibited an ultrahigh water/salt selectivity of up to 5196. This water/NaCl separation performance also exceeds those of most reported membranes (Fig. 5c)[12, 20, 41–43].

3 Materials and methods

3.1 Materials

Aluminum (III) nitrate nonahydrate ($Al(NO_3)_3·9H_2O$) was purchased from Shanghai Energy Chemical Co., Ltd. (Shanghai, China). 2-Aminoterephtalic acid (2-NH_2-BDC) was ob-

DOI: 10.52396/JUSTC-2024-0016
JUSTC, **2024**, 54(6): 0606

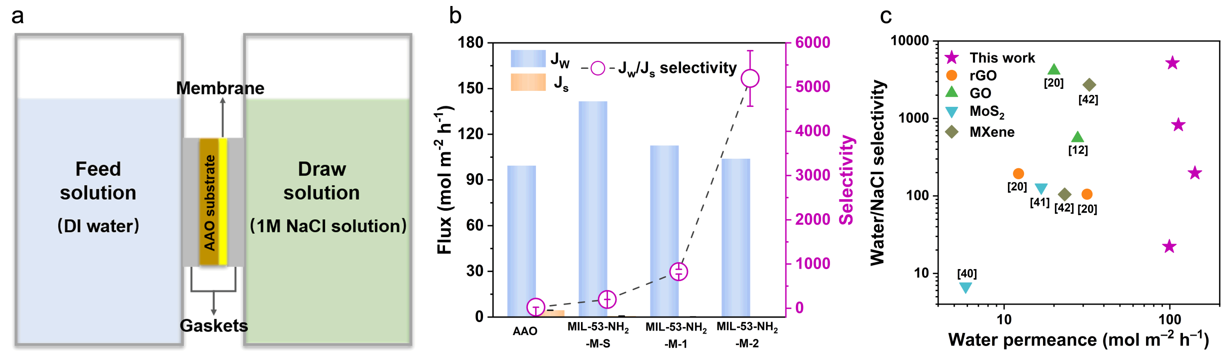

Fig. 5. Desalination performance of MIL-53(Al)-NH_2 membranes. (a) The homemade U-cell device for the tests of desalination performance. (b) The flux and selectivity of the AAO substrate and MIL-53(Al)-NH_2 membranes. (c) Comparison of MIL-53-NH_2-M-2 membranes with state-of-the-art membranes reported for water/NaCl separation in terms of permeance versus selectivity.

tained from TCI Development Co., Ltd. (Shanghai, China). *N*,*N*-dimethylformamide (DMF, 99.5%), acetic acid (CH_3COOH, 99.5%), ethanol (C_2H_5OH, 99.7%), NaCl, LiCl, $CaCl_2$, and $MgCl_2$ were of analytical grade and obtained from China National Pharmaceutical Group Industry Co. Ltd. (Beijing, China). All reagents and solvents were commercially available and used as received. Deionized (DI) water was used throughout the experiments.

Anodic alumina oxide (AAO, Hefei Pu-Yuan Nano Technology Ltd.) disks were used as substrates to support the MIL-53(Al)-NH_2 membranes.

3.2 Fabrication of the MIL-53(Al)-NH_2 membrane

3.2.1 The seeding preparation

An AAO substrate with a pore size of 90 nm±10 nm and a diameter of 25 mm was pretreated with 2-NH_2-BDC to grow a seed layer. First, 0.3 g of 2-NH_2-BDC, 80 mL of water, and 0.5 mL of CH_3COOH were added to a vial and stirred vigorously. Then, the solution was transferred into a Teflon vial containing an AAO substrate that was fixed on a self-designed Teflon holder vertically. The entire Teflon device was immersed in the reaction solution. The vial was sealed for pretreatment at 130 °C for 30 min and then cooled to room temperature. The obtained membrane was named MIL-53-NH_2-M-S.

3.2.2 The second growth for the fabrication of the MIL-53(Al)-NH_2 membrane

The Teflon device with the AAO substrate was removed from the pretreatment solution in step 1. $Al(NO_3)_3 \cdot 9H_2O$ (1.0 g) and 2-NH_2-BDC (0.3 g) were added to 80 mL of water. The solution was stirred and poured into another Teflon vial. The Teflon device with the AAO substrate was immersed in the solution. After 30 min/60 min at 80 °C, the membrane was removed after the solution cooled to room temperature. The MIL-53(Al)-NH_2 membrane was washed with ethanol 3 times and then stored in ethanol before use. Here, MIL-53(Al)-NH_2 membranes grown for 30 min and 60 min were named MIL-53-NH_2-M-1 and MIL-53-NH_2-M-2, respectively.

3.3 Fabrication of MIL-53(Al)-NH_2 powders

$Al(NO_3)_3 \cdot 9H_2O$ (1.0 g), 2-NH_2-BDC (0.3 g), and water (80 mL) were added to a Teflon vial. Then, the mixture was heated at 80 °C for 30 min/60 min in an oven. The MIL-53(Al)-NH_2 powders were collected via centrifugation and alternately washed with DMF and ethanol six times. The obtained powders were dried at 80 °C for 12 h. Here, the MIL-53(Al)-NH_2 powders synthesized for 30 min and 60 min were named MIL-53-NH_2-P-1 and MIL-53-NH_2-P-2, respectively.

3.4 MIL-53(Al)-NH_2 membrane characterization

3.4.1 Membrane structure characterization

Surface and cross-sectional images of the MIL-53(Al)-NH_2 membranes were obtained using field-emission scanning electron microscopy (SEM, Gemini500, Germany). The chemical structure of the MIL-53(Al)-NH_2 membranes was studied using a Fourier transform infrared spectrometer in attenuated total reflectance mode (FTIR-ATR, Thermo Nicolet FTIR spectrometer, USA).

3.4.2 Measurement of Na^+/Ca^{2+} and Li^+/Mg^{2+} separation performance under a concentration gradient

The ion separation performances of the AAO substrates MIL-53-NH_2-M-S, MIL-53-NH_2-M-1, and MIL-53-NH_2-M-2 were measured using a U-cell device (Fig. 4a) under a concentration gradient. The test membrane was mounted on the middle of the device, which separated the feed chamber and permeate chamber. Notably, the MOF layer side faced the feed chamber. In the feed chamber, the electrolyte solution (1 mol·L^{-1} NaCl, LiCl, $CaCl_2$, or $MgCl_2$) was used as the initial solution. Then, DI water was added to the permeate chamber. For MIL-53-NH_2-M-S and MIL-53-NH_2-M-1, the tests lasted for 30 min. For MIL-53-NH_2-M-2, the tests were extended to 1 h–3 h because of its extremely low ion permeation rates. After each test, the samples were drawn from the permeate chamber for inductively coupled plasma–optical emission spectrometry (ICP–OES, iCAP 7400) analysis to determine the ion concentration. Then, the device was thoroughly washed with DI water 3 times for 10 min each. The effective membrane area (A_m) was 1.13 cm^2. For each test, the samples were tested at least 3 times to obtain the average value.

The ion permeation rate ($J_{N^{n+}}$, mol·m^{-2}·h^{-1}) was measured by the ion concentration change in the permeation chamber and was calculated as follows:

$$J_{N^{n+}} = \frac{(C_t - C_0) \cdot V}{A_m \cdot t}, \tag{1}$$

where C_0 and C_t represent the molar concentrations (mol·L^{-1}) of the ion (N^{n+}) in the permeate chamber at the beginning (t = 0 h) and the end (t = 1 h), respectively. V is the volume of solution in the permeate chamber (15 mL).

The ideal ion selectivity of the membrane was calculated by the following equation:

$$S_{M^+/D^{2+}} = \frac{J_{M^+}}{J_{D^{2+}}}, \tag{2}$$

where J_{M^+} is the permeation rate of monovalent cations (Na^+ or Li^+) and $J_{D^{2+}}$ is the permeation rate of divalent cations (Ca^{2+} or Mg^{2+}).

3.4.3 Measurement of desalination performance under a concentration gradient

The desalination performances of the AAO substrates MIL-53-NH_2-M-S, MIL-53-NH_2-M-1, and MIL-53-NH_2-M-2 were measured using the same device used for the ion separation measurements. The test membrane was installed to separate the feed side and draw side (Fig. 5a). Notably, the MOF layer faced the draw side. Fifteen milliliters of DI water was used as the feed solution on the feed side, and the electrolyte solution (i.e., 15 mL of 1 mol·L^{-1} NaCl) was used as the initial draw solution. The experiment was carried out for 5 h for each membrane. After each test, all the liquid in the feed solution was drawn from the feed side for weighing, and part of the liquid was collected for inductively coupled plasma–optical emission spectrometry (ICP–OES, iCAP 7400) analysis. Then, the device was thoroughly washed with DI water 3 times for 10 min each. The effective membrane area ($A_{\rm m}$) was 1.13 cm^2.

The water ($J_{\rm w}$, mol·m^{-2}·h^{-1}) and salt permeation rates ($J_{\rm s}$, mol·m^{-2}·h^{-1}) were calculated as follows:

$$J_{\rm w} = \frac{\rho \cdot \Delta V}{A_m \cdot t \cdot M_{\rm w}}, \tag{3}$$

$$J_{\rm s} = \frac{C_t V_t - C_0 V_0}{A_m \cdot t}, \tag{4}$$

where ρ(g·L^{-1}) is the density of water, ΔV (mL) is the volume change on the feed side, and C_0 (mol·L^{-1}) and C_t (mol·L^{-1}) are the initial and final salt concentrations on the feed side at the beginning (t = 0 h) and the end (t = 5 h), respectively. V_0 (mL) and V_t (mL) are the initial and final volumes of DI water, respectively. $M_{\rm w}$ (g·mol^{-1}) is the molecular weight of water.

4 Conclusions

In summary, MIL-53(Al)-NH_2 membranes with angstrom-scale (~7 Å) channels for ion selective transport were fabricated by a simple and fast secondary growth method. Such membranes containing intrinsic angstrom-scale channels allow the entry of smaller monovalent ions and molecules, despite the dense growth of MIL-53(Al)-NH_2 on the support. For example, Na^+ and Li^+ can pass through the MOF layer 2 orders of magnitude faster than other slightly larger ions (i.e., Ca^{2+} and Mg^{2+}), playing a regulatory role in cation selectivity. Therefore, the resultant MIL-53(Al)-NH_2 membranes show high selectivities of 121.42 and 93.81 for Na^+/Mg^{2+} and Li^+/Mg^{2+}, respectively. Additional desalination experiments showed excellent water/salt selectivity up to 5196. This work confirms that MOFs facilitate further implementation of these ion and molecular separation processes and may stimulate the research and development of MOF-based membranes.

Acknowledgements

This work was supported by the Fundamental Research Funds for the Central Universities (WK2060000030), USTC Research Funds of the Double First Class Initiative (YD2060002022), and Major Science and Technology Innovation Projects in Shandong Province (2022CXGC020415).

Conflict of interest

The authors declare that they have no conflict of interest.

Biographies

Wenmin Li is currently a master's student at the School of Chemistry and Materials Science, University of Science and Technology of China, under the supervision of Prof. Tongwen Xu. Her research mainly focuses on metal-organic framework membranes for ion separation.

Tingting Xu is currently an Associate Research Fellow at the University of Science and Technology of China (USTC). She received her Ph.D. degree from USTC in 2020. Her research interests include the fabrication of advanced porous material membranes and their separation mechanism.

Tongwen Xu is currently a Professor at the University of Science and Technology of China. He received his Ph.D. degree from Tianjin University in 1995. His research interests cover membranes and related processes, particularly ion exchange membranes and membranes for energy and environmental applications.

References

[1] Song J F, Nghiem L D, Li X M, et al. Lithium extraction from Chinese salt-lake brines: opportunities, challenges, and future outlook. *Environ. Sci. : Water Res. Technol.*, **2017**, *3* (4): 593–597.

[2] Delmas C. Sodium and sodium-ion batteries: 50 years of research. *Adv. Energy. Mater.*, **2018**, *8* (17): 1703137.

[3] Liu Z X, Huang Y, Huang Y, et al. Voltage issue of aqueous rechargeable metal-ion batteries. *Chem. Soc. Rev.*, **2020**, *49* (1): 180–232.

[4] Li J L, Fleetwood J, Hawley W B, et al. From materials to cell: state-of-the-art and prospective technologies for lithium-ion battery electrode processing. *Chem. Rev.*, **2022**, *122* (1): 903–956.

[5] Nightingale Jr E R. Phenomenological theory of ion solvation. Effective radii of hydrated ions. *J. Phys. Chem.*, **1959**, *63* (9): 1381–1387.

[6] Tansel B, Sager J, Rector T, et al. Significance of hydrated radius and hydration shells on ionic permeability during nanofiltration in dead end and cross flow modes. *Sep. Purif. Technol.*, **2006**, *51* (1): 40–47.

[7] Guo Y, Ying Y L, Mao Y Y, et al. Polystyrene sulfonate threaded through a metal–organic framework membrane for fast and selective lithium-ion separation. *Angew. Chem. Int. Ed.*, **2016**, *55* (48): 15120–15124.

[8] Lu J, Zhang H C, Hou J, et al. Efficient metal ion sieving in rectifying subnanochannels enabled by metal–organic frameworks.

Nat. Mater., **2020**, *19* (7): 767–774.
[9] Zhang Y, Wang L, Sun W, et al. Membrane technologies for Li^+/Mg^{2+} separation from salt-lake brines and seawater: A comprehensive review. *J. Ind. Eng. Chem.*, **2020**, *81*: 7–23.
[10] Peng H W, Zhao Q. A Nano-Heterogeneous membrane for efficient separation of lithium from high magnesium/lithium ratio brine. *Adv. Funct. Mater.*, **2021**, *31* (14): 2009430.
[11] Sun Y, Wang Q, Wang Y H, et al. Recent advances in magnesium/lithium separation and lithium extraction technologies from salt lake brine. *Sep. Purif. Technol.*, **2021**, *256*: 117807.
[12] Abraham J, Vasu K S, Williams C D, et al. Tunable sieving of ions using graphene oxide membranes. *Nat. Nanotechnol.*, **2017**, *12* (6): 546–550.
[13] Dou H Z, Xu M, Wang B Y, et al. Microporous framework membranes for precise molecule/ion separations. *Chem. Soc. Rev.*, **2021**, *50* (2): 986–1029.
[14] Kang J, Ko Y, Kim J P, et al. Microwave-assisted design of nanoporous graphene membrane for ultrafast and switchable organic solvent nanofiltration. *Nat. Commun.*, **2023**, *14* (1): 901.
[15] O'Hern S C, Boutilier M S H, Idrobo J C, et al. Selective ionic transport through tunable subnanometer pores in single-layer graphene membranes. *Nano Lett.*, **2014**, *14* (3): 1234–1241.
[16] Ayyaru S, Ahn Y H. Application of sulfonic acid group functionalized graphene oxide to improve hydrophilicity, permeability, and antifouling of PVDF nanocomposite ultrafiltration membranes. *J. Membr. Sci.*, **2017**, *525*: 210–219.
[17] Wang M D, Zhang P H, Liang X, et al. Ultrafast seawater desalination with covalent organic framework membranes. *Nat. Sustain.*, **2022**, *5* (6): 518–526.
[18] Cassady H J, Cimino E C, Kumar M, et al. Specific ion effects on the permselectivity of sulfonated poly(ether sulfone) cation exchange membranes. *J. Membr. Sci.*, **2016**, *508*: 146–152.
[19] Geng K Y, He T, Liu R Y, et al. Covalent organic frameworks: design, synthesis, and functions. *Chem. Rev.*, **2020**, *120* (16): 8814–8933.
[20] Chen L, Shi G S, Shen J, et al. Ion sieving in graphene oxide membranes via cationic control of interlayer spacing. *Nature*, **2017**, *550* (7676): 380–383.
[21] Zhang H C, Hou J, Hu Y X, et al. Ultrafast selective transport of alkali metal ions in metal organic frameworks with subnanometer pores. *Sci. Adv.*, **2018**, *4* (2): eaaq0066.
[22] Hou J, Zhang H C, Simon G P, et al. Polycrystalline advanced microporous framework membranes for efficient separation of small molecules and ions. *Adv. Mater.*, **2020**, *32* (18): 1902009.
[23] Ran J, Wu L, He Y B, et al. Ion exchange membranes: New developments and applications. *J. Membr. Sci.*, **2017**, *522*: 267–291.
[24] Zhao D L, Japip S, Zhang Y, et al. Emerging thin-film nanocomposite (TFN) membranes for reverse osmosis: A review. *Water Res.*, **2020**, *173*: 115557.
[25] Yadav D, Karki S, Ingole P G. Current advances and opportunities in the development of nanofiltration (NF) membranes in the area of wastewater treatment, water desalination, biotechnological and pharmaceutical applications. *J. Environ. Chem. Eng.*, **2022**, *10* (4): 108109.
[26] Denny Jr M S, Moreton J C, Benz L, et al. Metal–organic frameworks for membrane-based separations. *Nat. Rev. Mater.*, **2016**, *1*: 16078.
[27] Zhao X, Wang Y X, Li D S, et al. Metal–organic frameworks for separation. *Adv. Mater.*, **2018**, *30* (37): 1705189
[28] Yu S J, Pang H W, Huang S Y, et al. Recent advances in metal–organic framework membranes for water treatment: A review. *Sci. Total. Environ.*, **2021**, *800*: 149662.
[29] Liu Y C, Yeh L H, Zheng M J, et al. Highly selective and high-performance osmotic power generators in subnanochannel membranes enabled by metal-organic frameworks. *Sci. Adv.*, **2021**, *7* (10): eabe9924.
[30] Li X Y, Zhang H C, Yu H, et al. Unidirectional and selective proton transport in artificial heterostructured nanochannels with nano-to-subnano confined water clusters. *Adv. Mater.*, **2020**, *32* (24): 2001777.
[31] Li X Y, Zhang H C, Wang P Y, et al. Fast and selective fluoride ion conduction in sub-1-nanometer metal-organic framework channels. *Nat. Commun.*, **2019**, *10*: 2490.
[32] Qian T Y, Zhang H C, Li X Y, et al. Efficient gating of ion transport in three-dimensional metal–organic framework sub-nanochannels with confined light-responsive azobenzene molecules. *Angew. Chem. Int. Ed.*, **2020**, *59* (31): 13051–13056.
[33] Jian M P, Qiu R S, Xia Y, et al. Ultrathin water-stable metal-organic framework membranes for ion separation. *Sci. Adv.*, **2020**, *6* (23): eaay3998.
[34] Xu T T, Shehzad M A, Yu D B, et al. Highly cation permselective metal–organic framework membranes with leaf-like morphology. *ChemSusChem*, **2019**, *12* (12): 2593–2597.
[35] Tran T V, Jalil A A, Nguyen D T C, et al. A critical review on the synthesis of NH_2-MIL-53(Al) based materials for detection and removal of hazardous pollutants. *Environ. Res.*, **2023**, *216*: 114422.
[36] Zeng F M, Yang Y H, Li X H, et al. Ionic sieving at sub-angstrom precision enabled by metal organic frameworks. *ACS Appl. Mater. Interfaces*, **2023**, *15* (34): 40839–40845.
[37] Li H Z, Qiu C L, Ren S J, et al. Na^+-gated water-conducting nanochannels for boosting CO_2 conversion to liquid fuels. *Science*, **2020**, *367* (6478): 667–671.
[38] Sorribas S, Gorgojo P, Téllez C, et al. High flux thin film nanocomposite membranes based on metal–organic frameworks for organic solvent nanofiltration. *J. Am. Chem. Soc.*, **2013**, *135* (40): 15201–15208.
[39] Lu X Y, Geng Y Z, Jia Z Q, et al. In situ syntheses of NH_2-MIL-53/PVDF composite membranes for dyes separation. *Sep. Purif. Technol.*, **2021**, *269*: 118760.
[40] Chin J M, Chen E Y, Menon A G, et al. Tuning the aspect ratio of NH_2-MIL-53(Al) microneedles and nanorods via coordination modulation. *CrystEngComm*, **2013**, *15* (4): 654–657.
[41] Deng M M, Kwac K, Li M, et al. Stability, molecular sieving, and ion diffusion selectivity of a lamellar membrane from two-dimensional molybdenum disulfide. *Nano Lett.*, **2017**, *17* (4): 2342–2348.
[42] Hirunpinyopas W, Prestat E, Worrall S D, et al. Desalination and nanofiltration through functionalized laminar MoS_2 membranes. *ACS Nano*, **2017**, *11* (11): 11082–11090.
[43] Lu Z, Wei Y Y, Deng J J, et al. Self-crosslinked MXene ($Ti_3C_2T_x$) membranes with good antiswelling property for monovalent metal ion exclusion. *ACS Nano*, **2019**, *13* (9): 10535–10544.

DOI: 10.52396/JUSTC-2024-0016
JUSTC, **2024**, 54(6): 0606